COBEM 2021 26th International Congress of Mechanical Engineering
November 22-26, 2021, Virtual Congress, Brazil
ABCM Associação Brasileira de Engenharia e Ciências Mecânicas

COB-2021-0930
A BRIEF REVIEW OF WALL SHEAR CORRELATIONS FOR HYPERSONIC FLOWS

Pedro Paulo Batista de Araújo
Felipe Pinheiro Maia
Jonatha Wallace da Silva Araújo
Ítalo Sabino Arrais Bezerra
Paulo Gilberto de Paula Toro
Sandi Itamar Schafer de Souza
Thiago Cardoso de Souza
Federal University of Rio Grande do Norte, Department of Mechanical Engineering, Natal, Postal Code 59072-970, Brazil
araujo.projects@gmail.com, felipepm99@hotmail.com, jonatha_wallace@hotmail.com, italosb94@hotmail.com, toro11pt@gmail.com, sandi@ufrn.br, thiago.souza@ufrn.br

Ramon Carneiro
Aeronautics Institute of Technology, Aerospace Science and Technology Graduate Program, São José dos Campos, Postal Code 12228-900, Brazil.
ramon_cgd@hotmail.com

Abstract. *This paper adresses the problem of finding the appropriate correlation model for the estimation of drag force in aerospace vehicles that operate at hypersonic conditions. Here the analysis of the spatial variation of the local wall shear stress along a 6.28° ramp wall in a hypersonic flow is considered. Three cases corresponding to flows with Mach numbers equal to 3, 7, and 10 were analyzed. A number of correlations of the friction coefficient as proposed by Sommer and Short, Spalding and Chi, van Driest, White and Christoph, Eckert, and Meador and Smart, were applied to evaluate the wall shear using an analytical approach. The thermodynamic properties of the flow downstream of the shock wave, established at the leading edge of the ramp, were estimated using the oblique shock theory. The analytical results were compared to a reference wall shear data numerically obtained using a Reynolds-Averaged Navier-Stokes (RANS) steady-state simulation performed for the same geometry. The working fluid is air, modeled in this paper as a calorically perfect gas. For the closure of the turbulent Reynolds stresses, the k-kl-ω transition model was used. The results show a quantitative comparison between the wall shear stress curves obtained for each method and correlation introduced. The results points out that most correlations models have low accuracy for the hypersonic flow, which is reasonable since these models were developed from experimental data extracted from supersonic flows. Despite this limitation, the analytical models which best predict the drag coefficient under the conditions investigated were the models derived by Eckert, the model proposed by Sommer and Short for supersonic flows and the Meador and Smart model for hypersonic flow.*

Keywords: *Skin Friction Drag, Wall Shear Stress, CFD, Analytical Correlations Models, Hypersonic Flow*

1. INTRODUCTION

Airbreathing Supersonic Combustion (scramjet) technology is one of the most promising alternatives for space access propulsion. Scramjet is an engine that uses its geometry to compress the atmospheric air at the compression section (inlet) by creating a set of oblique shock waves and keeping the flow supersonic at the combustion chamber. One of the main aspects of an aerospace vehicle is the aerodynamic drag, a parameter that is essential for predicting flight trajectories.

The aerodynamic drag is a force that acts in the opposite direction to the flow, resisting body movement. It is commonly divided into components related to pressure and the viscous friction. While the pressure drag can be easily computed or even experimentally obtained, the friction drag depends directly on the shear stresses developed on the vehicle surface due to the boundary layer flow near the wall. It is, therefore, a property that depends on the boundary layer velocity profile, a characteristic difficult to estimate a priori, especially in the case of supersonic or hypersonic flows (Wang *et al.*, 2017).

There are different methods to estimate the wall shear stress for the flow past a solid surface, these methods are generally classified between CFD and analytical correlations. The first one numerically calculates the velocity flow field, but it is expensive and requires a long time for the appropriate analysis of the flow. Analytical correlations, on the other hand, tend to lose accuracy for analysis conditions which are different from those experimentally obtained. Several correlations can be obtained in the literature for hypersonic flow over aerospace vehicles. Thus, scramjet designers and

researchers are interested in understanding which model is the best to estimate the shear on the scramjet compression ramps for a given flow condition.

With the growing capability of the numerical analysis of hypersonic flows, it has been observed that many published works are based on a sort of mixing involving the two approaches, using the large amount of data that can be extracted from computer simulations to develop direct relationships for a given flow. For example, Kshetrimayum *et al.* (2020) studied the wall shear stress development in situations associated with the formation of recirculating secondary flows arising due to shock wave-boundary layer interactions. A large number of numerical studied are based on developing correlations that can predict the averaged wall shear. In the same way, Grasso *et al.* (2021) applied unsteady CFD modelling to predict the pressure distribution over an airfoil. Kumar *et al.* (2018) presented a correlation for the Nusselt number, Nu, and form factor obtained using CFD to predict the heat transfer in triangular solar heaters duct. These examples show both the versatility of numerical methods and their accuracy in predicting the physical phenomena.

In this sense, the present work aims to evaluate the accuracy of some analytical correlations used to predict the wall shear stress on a simple wedge subjected to an upstream hypersonic flow and to compare these correlations with the data obtained.

2. LITERATURE REVIEW

In this section, a brief review of the correlation models used for calculating the friction coefficient, c_f, for compressible turbulent flows over a flat plate will be briefly exposed. In general, these correlations were developed between the 60's and 80's from experimental data obtained for compressible supersonic flows. White and Christoph (1971) established that the existing correlations for the friction coefficient, over a flat plate, can be obtained from the already existing relations obtained for incompressible flows, by carefully considering a correction in the Reynolds number. The generic format for this type of correlation is given by:

$$c_{f,\,\text{compr}} = \frac{1}{F_c} c_{f,\,\text{in}} \left(R_x F_{R,x}\right) \tag{1}$$

where $c_{f,\,\text{compr}}$ and $c_{f,\,\text{in}}$ are the friction coefficients for the turbulent compressible and incompressible cases, respectively. R_x is the local Reynolds number, F_c is the transformation function applied to the correlation for incompressible case and $F_{R,x}$ is the correction function of the Reynolds number.

For turbulent incompressible flow, one can adopt the model proposed by White and Christoph (1971).

$$c_{f,\,\text{in}} = \frac{0.451}{\ln^2\left(0.056 R_x\right)} \tag{2}$$

A more general expression for c_f is the one proposed by White and Christoph (1971).

$$c_{f,\,\text{compr}} = \frac{T_e}{T_w} f^2 c_{f,\,\text{in}} \left[R_x f \left(\frac{T_e}{T_w}\right)^{n+1}\right], \quad f = \frac{1 + 0.044 r M_e^2 \left(T_e/T_w\right)}{1 + 0.3\left(T_{aw}/T_w - 1\right)} \tag{3}$$

where T_e, T_w, and T_{aw} are the fluid temperature outside the boundary layer, the wall temperature, and the adiabatic wall temperature, respectively. M_e is the Mach number, n is a constant equal to 0.67 for air, and r is the adiabatic recovery factor, which is 0.89 for turbulent flows. Other correlations are presented by van Driest (1956) and Spalding and Chi (1964). Both correlations use the same transformation function (Eq. 4), however the Reynolds number correction is different in each case (Eqs. 5 and 6, respectively).

$$F_c = \frac{0.2 r M_e^2}{\left[\sin^{-1}\left(\frac{2a^2 - b}{4a^2 + b^2}\right)^{1/2} + \sin^{-1}\frac{b}{\left(4a^2 + b^2\right)^{1/2}}\right]^2}, \quad a = \left(0.2 r M_e^2 \frac{T_e}{T_w}\right)^{1/2} \text{ and } \quad b = \frac{T_e}{T_w}\left(1 + 0.044 r M_e^2 - \frac{T_w}{T_e}\right) \tag{4}$$

$$F_{R,\,x,\,\textit{van Driest}} = \left(\frac{T_e}{T_w}\right)^n \tag{5}$$

$$F_{R,\,x,\,\textit{Spalding and Chi}} = \left(\frac{T_e}{T_w}\right)^{0.702} \left(\frac{T_w}{T_{aw}}\right)^{0.772} \tag{6}$$

Two other correlation proposals take into account a reference temperature (T^*) for the calculation at different wall temperatures. Both Eckert (1955) and Sommer and Short (1955) present the calculation of the friction coefficient in the compressible turbulent flow, these correlations differ from each other only in the values of the constants C_1, C_2 and C_3.

$$c_{f,\,\text{compr}} = \frac{T_e}{T^*} c_{f,\,\text{in}} \left[R_x \left(\frac{T_e}{T^*} \right)^{n+1} \right], \quad T^* = T_e \left(C_1 + C_2 \left(\frac{\gamma - 1}{2} \right) r M_e^2 + C_3 \frac{T_w}{T_e} \right) \tag{7}$$

where C_1 = 0.5, C_2 = 0.22 and C_3 = 0.5 for Eckert (1955) and C_1 = 0.55, C_2 = 0.197 and C_3 = 0.45 for Sommer and Short (1955). As Sommer and Short (1955) proposed, correcting constants from previously published models is a viable option for the development of new correlations.

Finally, Meador and Smart (2005) present a more recent study on correlations, suggesting a new constant C_2 for the reference temperature expression, in this case, equal to 0.16. In this case the expression of the friction drag coefficient for the compressible turbulent flow.

$$c_{f,\,\text{compr},\,\textit{Meador and Smart}} = \frac{0.02296}{R_x^{0.139}} \left(\frac{\rho^*}{\rho_e} \right)^{0.861} \left(\frac{\mu^*}{\mu_e} \right)^{0.139} \tag{8}$$

where ρ_e and ρ^* are the fluid density outside the boundary layer and the reference density, μ_e is the dynamic viscosity outside the boundary layer, and μ^* is the reference dynamic viscosity.

3. NUMERICAL EXPERIMENT

Differents cases were numerically analyzed with the use of the commercial CFD solver *Ansys FLUENT*. A series of numerical experiments were performed to obtain a reference database for the shear stress in a ramp submitted to a hypersonic flow. Three cases were analyzed and are considered as a reference in more detail the supersonic flow over a wedge at velocities corresponding to a Mach number of 3, 7 and 10 at 30 km altitude. The selected geometry is a ramp of 500 mm length and an angle of 6.28°, corresponding to the first ramp of the scramjet geometry as presented in Araújo (2019); Carneiro (2020); Bezerra (2020). Furthermore, a domain with 150 mm height and a 20 mm entry section upstream of the ramp's leading edge was adopted (Fig. 1).

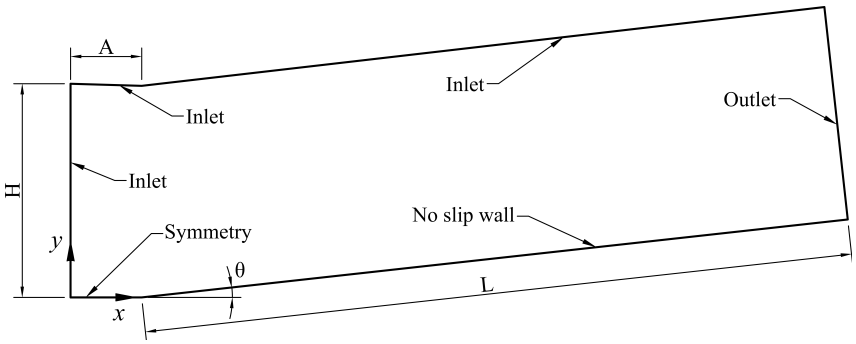

Figure 1. Computational domain used in the CFD analysis. In this case, H = 150 mm, L = 500 mm, A = 5 mm e θ= 6.28°.

The domain (Fig. 1) was discretized using a set of quadrilateral elements forming a structured mesh in Cartesian coordinates, this is illustrated by Figure 2. An extensive near wall refinement is imposed in order to guarantee the required wall condition ($y^+ < 1$) capture the flow effects due to the viscous sublayer effects. Refinement is also applied towards the leading and trailing edges, since in these regions there is a sudden change in the geometry and, therefore, in the pattern of the flow.

RANS (Reynolds Average Navier-Stokes) simulations were performed considering a steady and compressible flow for all cases. The corresponding set of governing equations are given as follows (Versteeg and Malalasekera, 2007):

$$\frac{\partial \left(\overline{\rho}\, \tilde{u}_i \right)}{\partial x_i} = 0 \tag{9}$$

$$\frac{\partial \left(\overline{\rho}\, \tilde{u}_j\, \tilde{u}_i \right)}{\partial x_j} = -\frac{\partial \overline{p}}{\partial x_i} + \frac{\partial}{\partial x_j} \left[\left(\mu + \mu_t \right) \left(\frac{\partial \tilde{u}_i}{\partial x_j} + \frac{\partial \tilde{u}_j}{\partial x_i} \right) \right] + \frac{\partial}{\partial x_j} \left[\frac{1}{3} \left(\mu + \mu_t \right) \frac{\partial \tilde{u}_i}{\partial x_i} \delta_{ij} \right] \tag{10}$$

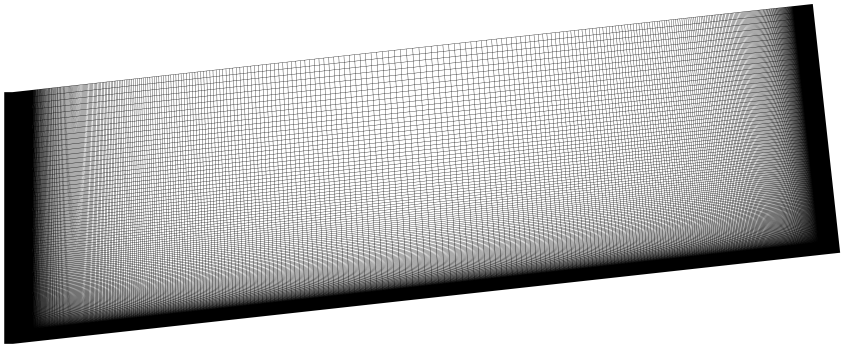

Figure 2. Mesh adopted for domain discretization.

$$\frac{\partial\left(\tilde{u}_j\,\tilde{T}\right)}{\partial x_j} = \frac{\partial}{\partial x_j}\left[\left(\alpha+\alpha_t\right)\frac{\partial\tilde{T}}{\partial x_j}\right] + \tilde{\phi} \tag{11}$$

where ρ is the density of the fluid, p the pressure, which is related to ρ in the compressible formulation through the ideal gas state equation: $p = \rho RT$ (R is the ideal gas constant). T is the temperature, and u_i the velocity field. The variable μ is the fluid viscosity, α the thermal diffusivity of the fluid, μ_t the turbulent viscosity, and α_t the turbulent thermal diffusivity. The term ϕ is the viscous dissipation, defined as:

$$\tilde{\phi} = -\frac{2}{3}\mu\left(\frac{\partial\tilde{u}_i}{\partial x_i}\right)^2 + \frac{\mu}{2}\left(\frac{\partial\tilde{u}_j}{\partial x_i}+\frac{\partial\tilde{u}_i}{\partial x_j}\right)\left(\frac{\partial\tilde{u}_j}{\partial x_i}+\frac{\partial\tilde{u}_i}{\partial x_j}\right) \tag{12}$$

The index i and j assume values from 1 to 3. The overbar indicates a time-averaged variable and the tilde indicates a Favre-averaged variable (Versteeg and Malalasekera, 2007).

The hypothesis of air as a calorically perfect gas was assumed to evaluate the fluid density. For the closure of the turbulent viscosity, the turbulent model *k-kl-ω* was adopted. This model adds three transport equations to the set given by Eq. 9-11, in this case, the equations for the laminar kinetic energy (k_L), the turbulent kinetic energy (k_T), and the viscous dissipation rate (ω), here presented in Eqs. 13-15. This model is capable of capturing the laminar and turbulent effects of the boundary layer, thereby predicting a consistent velocity gradient which forms in the near wall flow. More details can be found at Walters and Cokljat (2008).

$$\frac{\partial\left(\rho k_T u_j\right)}{\partial x_j} = \rho\left(P_{k_T} + R_{\text{BP}} + R_{\text{NAT}} - \omega k_T - D_T\right) + \frac{\partial}{\partial x_j}\left[\left(\mu+\frac{\rho\alpha_T}{\sigma_k}\right)\frac{\partial k_T}{\partial x_j}\right] \tag{13}$$

$$\frac{\partial\left(\rho k_L u_j\right)}{\partial x_j} = \rho\left(P_{k_L} + R_{\text{BP}} + R_{\text{NAT}} - D_L\right) + \frac{\partial}{\partial x_j}\left(\mu\frac{\partial k_L}{\partial x_j}\right) \tag{14}$$

$$\frac{\partial\left(\rho\omega u_j\right)}{\partial x_j} = \rho\left[C_{\omega 1}\frac{\omega}{k_T}P_{k_T} + \left(\frac{C_{\omega R}}{f_W}-1\right)\frac{\omega}{k_T}\left(R_{\text{BP}}+R_{\text{NAT}}\right) - C_{\omega 2}\omega^2 + C_{\omega 3}f_\omega\alpha_T f_W^2\frac{\sqrt{k_T}}{d^3}\right] + \frac{\partial}{\partial x_j}\left[\left(\mu+\frac{\rho\alpha_T}{\sigma_\omega}\right)\frac{\partial\omega}{\partial x_j}\right] \tag{15}$$

In this study, the convective fluxes are modelled using the second order upwind Roe-FDS scheme, which is suitable for flows with the presence of a shock wave (Blazek, 2001). The Sutherland's law was used to the viscosity.

As boundary conditions, the non-slip condition for the wall is used, the wall is considered isothermal at 300 K. In the symmetry line shown in Figure 1, the symmetry condition is imposed. At the outlet, atmospheric pressure of 0 Pa and a temperature of 300 K were considered. In addition, the thermodynamic properties used for the inlet flow were obtained for an altitude of 30 km (NASA, 1976), according to Araújo (2019); Carneiro (2020); Bezerra (2020). Turbulent intensity of 5% was imposed in the inlet section. Such properties are summarized in Table 1. The only appreciable change between the cases was the Mach number, which was set equal to 3, 7 and 10 for the supersonic and hypersonic cases, respectively.

Table 1. Thermodynamic properties considered for the evaluation of the reference cases.

Pressure (Pa)	**Temperature (K)**	**Density (kg/m^3)**	**Speed of sound (m/s)**
1197	226.5	1.84×10^{-2}	301.7

The value of 10^{-5} was adopted as a convergence criterion for the averaged residuals of the numerical solution for all transport equations.

In order to check the independence of the numerical results with the resolution of the discretized domain shown in Fig. 2, the Grid Convergence Index (GCI) method was applied Celik *et al.* (2008). The three meshes selected for this study has the same y^+ parameter and in all cases the first layer thickness is set to have a distance of 10^{-3} mm from the wall. Figure 3 shows the downstream development of this parameter for the flow cases with Mach numbers 3, 7 and 10.

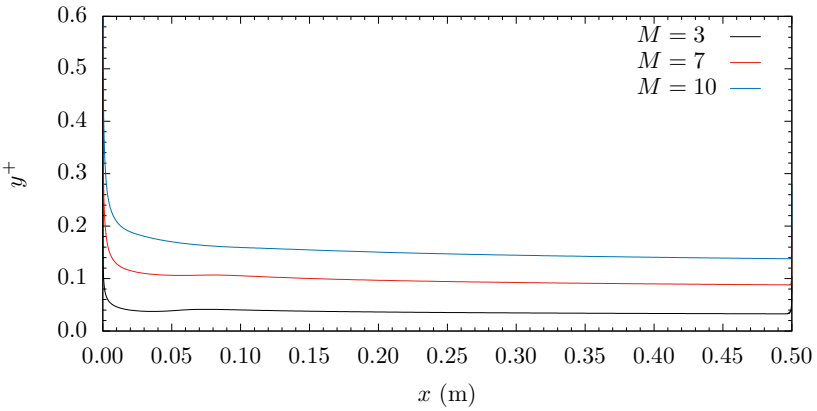

Figure 3. y^+ along the wall ramp.

In addition, this study intends to investigate the influence of the shockwave thickness in evaluation of the wall shear stress. The refinement ratio adopted between the meshes was $rr \approx 1.5$. Table 2 presents the number of elements of each mesh, and the GCI index calculated for different physical properties, e.g., pressure, temperature and the total drag.

Table 2. Grid Convergence Index analysis.

	Freestream Mach number		
	3	7	10
N_1	261000	261000	261000
N_2	116000	116000	116000
N_3	52650	52650	52650
rr_{21}	1.500	1.500	1.500
rr_{32}	1.484	1.484	1.484
Pressure			
GCI_{21}	5.738%	3.439%	0.956%
GCI_{32}	3.276%	5.307%	1.956%
Temperature			
GCI_{21}	0.207%	0.387%	0.005%
GCI_{32}	0.141%	0.176%	0.000%
Total drag			
GCI_{21}	0.062%	0.159%	0.153%
GCI_{32}	0.003%	0.005%	0.004%

The GCI index reveals that grid independence of the temperature and drag properties are already achieved with the meshes selected. The GCI calculated with the pressure data, however, suggest the selection of Mesh 1 (which has the best spatial resolution) in order to guarantee a GCI index less than 1%.

Figure 4 and 5 presents, for the three meshes, the Mach number as a function of the height at the outlet and the wall shear stress developed in the wall ramp.

As can be observed, independence of the results with the mesh resolutions adopted in this paper are established for all flow quantities relevant in the present investigation.

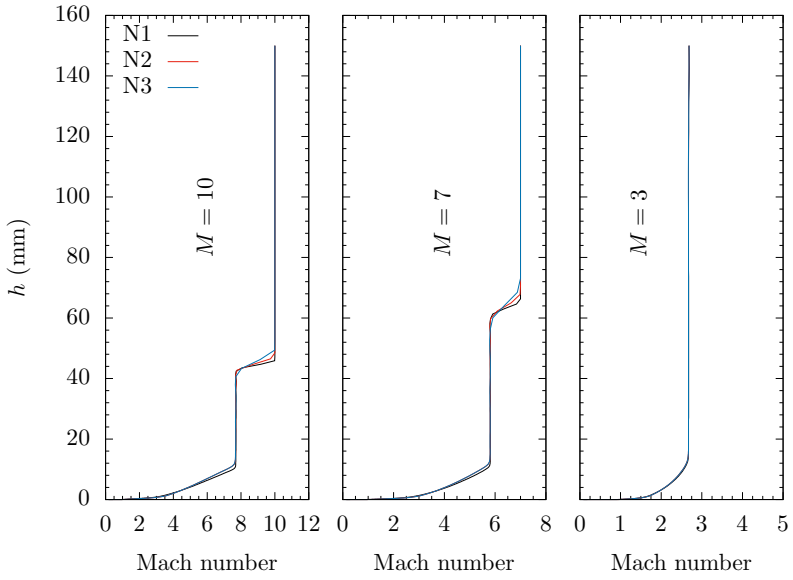

Figure 4. Mach number profile at the outlet, h represents the distance perpendicular to the wall.

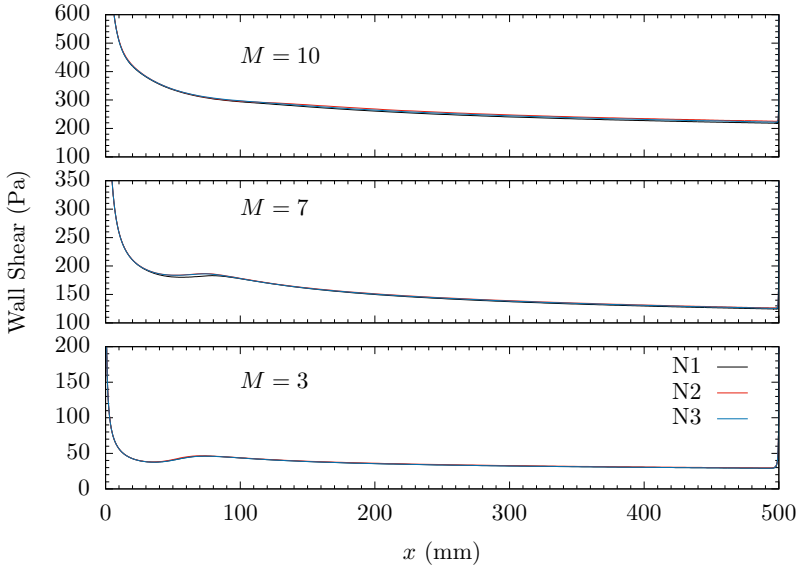

Figure 5. Wall Shear profile in the x-direction for different meshes and the corresponding freestream Mach number.

4. ANALYTICAL CORRELATIONS

To evaluate the aforementioned analytical correlations for the wall shear stress, the data obtained analytically using these correlations were compared with the numerical data obtained for the three cases. The first case is the supersonic flow (Mach number 3) and the second and third cases the hypersonic flows (Mach number 7 and 10).

Figures 6-8 show the results of the wall shear stresses along the ramp for all cases. The analytical analysis considered fully turbulent conditions, while the numerical simulation, as established in Section 3, predicts both the laminar and turbulent regions, and the region of transition. The location of the onset transition in each case analyzed is strongly dependent on the turbulent intensity imposed at the inlet section. In all the cases, the transition occurs before the first 100 mm of the ramp, with the case of Mach number 10 presenting a turbulent flow already at the leading edge. Since the analysis of the turbulent intensity was not the objective of this paper, the comparison between the wall shear stress curves only considers the turbulent part.

As can be seen in Figure 6, for flows with a relative lower Mach numbers (Mach number equal to 3), in general, the analytical correlations available in the literature represent the expected decay of the wall shear stress as the boundary layer develops further downstream. Relatively to the CFD model, the correlation that predicts a similar trend in this case, was the correlation expression derived by Sommer and Short (1955), followed the correlation obtained by Eckert (1955). As

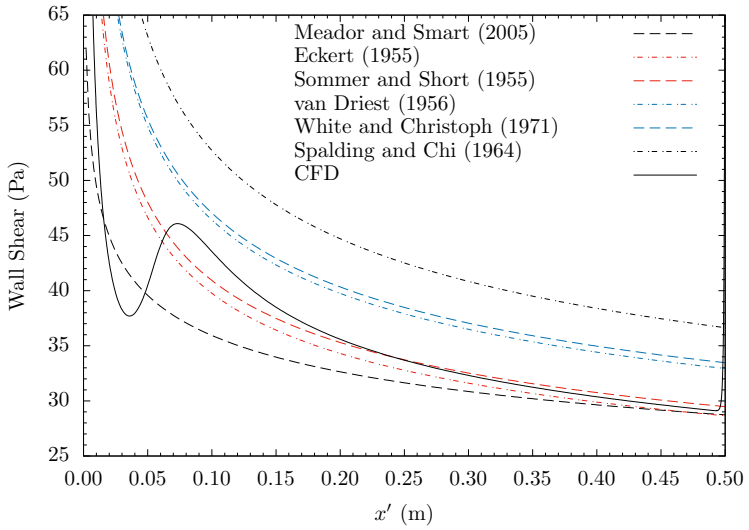

Figure 6. Wall shear curves over the ramp for flow corresponding to freestream Mach number 3.

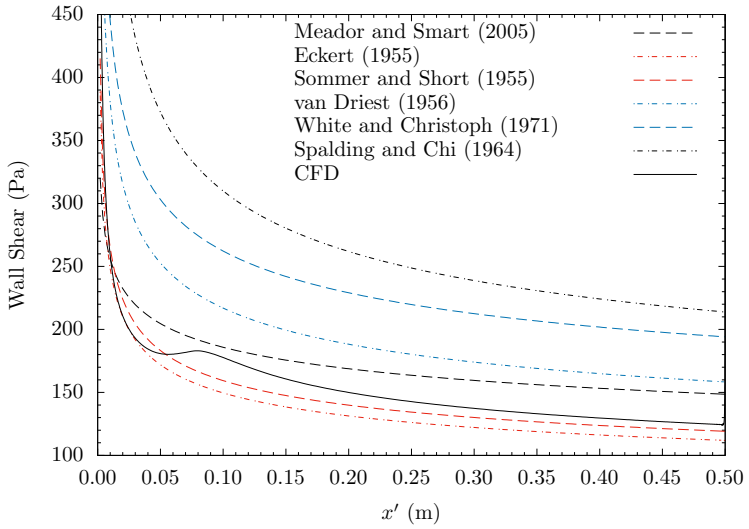

Figure 7. Wall shear curves over the ramp for flow corresponding to freestream Mach number 7.

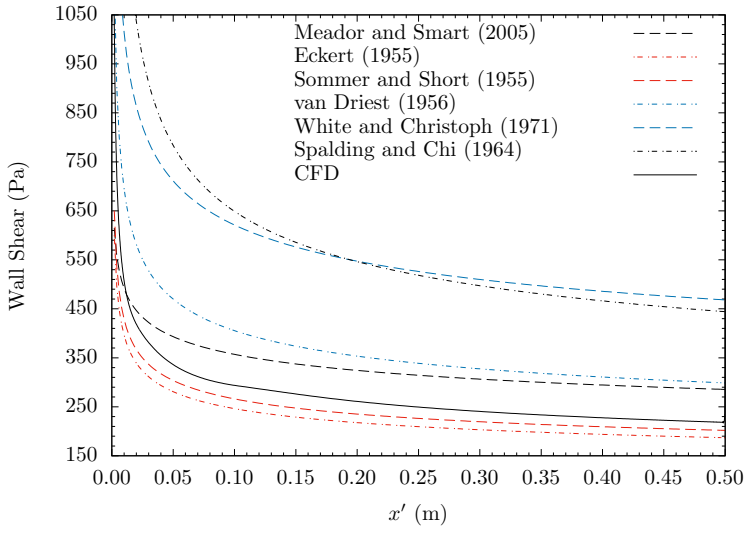

Figure 8. Wall shear curves over the ramp for flow corresponding to freestream Mach number 10.

the Mach number increases (Mach number equal to 7), reaching a hypersonic regime, the correlations of Sommer and Short (1955) and Eckert (1955) perform better than the others models, although with some underestimation of the wall shear. The model proposed by Meador and Smart (2005) also follows a similar trend as predicted by the CFD model.

Among the models reviewed in this article, an interesting feature seen in the works of Eckert (1955) and Sommer and Short (1955) is the possibility of proposing new models based on the correction of the constants of the existing models, which can be done using available experimental data in the literature or even data obtained numerically by RANS or LES simulations.

5. CONCLUSIONS

This work presents a review of some of the correlations available for predicting the drag in supersonic velocities. A case study was carried out using these analytical models, and a numerical study was used as a validation tool for reference. Based on the results obtained from the numerical experiments, it was concluded that:

1. For supersonic flow with Mach number equal to 3, the bests correlations observed were the Sommer and Short (1955) are those which closely follows the reference data.;
2. For hypersonic flows at Mach numbers 7 and 10, the three correlations that perform better are the correlations derived by Sommer and Short (1955) and Eckert (1955) and the correlation proposed by Meador and Smart (2005);
3. Sommer and Short (1955) and Meador and Smart (2005) employ the same equations used by Eckert (1955), changing the parameters to improve the model with the data available. Therefore, one could use CFD simulations to obtain data for differents hypersonic cases. Hence, a new CFD-based correlation could be proposed based on the Eckert model.

6. ACKNOWLEDGMENTS

This work was carried out with the support of the Academic Cooperation Program in National Defense (PROCAD-DEFENSE), grant 88881.387753/2019-01, and was financed in part by the Coordenação de Aperfeiçoamento de Pessoal de Nível Superior - Brasil (CAPES) - Finance Code 001. The authors would like to thank the Computational Fluid Dynamics Laboratory of the Federal University of Rio Grande do Norte (UFRN) for the infrastructure available. Additionally, the authors appreciate the support provided by the group of Hypersonic Flows ($GEH - UFRN$).

7. REFERENCES

Araújo, J.W.S., 2019. *Numerical analysis of the flow in the inlet section of a scramjet demonstrator. Análise numérica do escoamento na seção de captura de ar de um demonstrador scramjet*. Master dissertation (in Portuguese), Universidade Federal do Rio Grande do Norte, Natal-RN, Brazil.

Bezerra, I.S.A., 2020. *Numerical analysis of the influence of speed on supersonic combustion in a scramjet demonstrator*. Master dissertation (in Portuguese), Universidade Federal do Rio Grande do Norte, Natal-RN, Brazil.

Blazek, J., 2001. *Computational fluid dynamics: principles and applications*. Elsevier Science.

Carneiro, R., 2020. *Analytical study of the supersonic combustion technology demonstrator*. Master dissertation (in Portuguese), Universidade Federal do Rio Grande do Norte, Natal-RN, Brazil.

Celik, I.B., Ghia, U., Roache, P.J., Freitas, C.J., Coleman, H. and Raad, P.E., 2008. "Procedure for Estimation and Reporting of Uncertainty Due to Discretization in CFD Applications". *Journal of Fluids Engineering*, Vol. 130, No. 7. ISSN 0098-2202. doi:10.1115/1.2960953.

Eckert, E.R.G., 1955. "Engineering relations for heat transfer and friction in high-velocity laminar and turbulent boundary-layer flow over surfaces with constant pressure and temperature". *Journal of the Aeronautical Sciences*, Vol. 22, pp. 585–587.

Grasso, G., Wu, H., Orestano, S., Sanjosé, M., Moreau, S. and Roger, M., 2021. "Cfd-based prediction of wall-pressure spectra under a turbulent boundary layer with adverse pressure gradient". *CEAS Aeronautical Journal*, Vol. 12, No. 1, pp. 125–133. doi:10.1007/s13272-020-00484-5.

Kshetrimayum, M., Irimpan, K.J. and Menezes, V., 2020. "Skin friction estimation on a surface under shock-boundary layer interaction". *Sādhanā*, Vol. 45, No. 1, pp. 1–9. doi:10.1007/s12046-020-01437-8.

Kumar, R., Goel, V. and Kumar, A., 2018. "Investigation of heat transfer augmentation and friction factor in triangular duct solar air heater due to forward facing chamfered rectangular ribs: A cfd based analysis". *Renewable Energy*, Vol. 115, pp. 824–835. doi:10.1016/j.renene.2017.09.010.

Meador, W.E. and Smart, M.K., 2005. "Reference enthalpy method developed from solutions of the boundary-layer equations". *AIAA journal*, Vol. 43, No. 1, pp. 135–139.

NASA, 1976. "U.S. Standard Atmosphere". `https://ntrs.nasa.gov/search.jsp?R=19770009539`. Acessed on 2021-06-19.

Sommer, S.C. and Short, B.J., 1955. "Free-flight measurements of turbulent-boundary-layer skin friction in the presence of severe aerodynamic heating at mach numbers from 2.8 to 7.0".

Spalding, D. and Chi, S., 1964. "The drag of a compressible turbulent boundary layer on a smooth flat plate with and without heat transfer". *Journal of Fluid Mechanics*, Vol. 18, No. 1, pp. 117–143.

van Driest, E.R., 1956. *The problem of aerodynamic heating*. Institute of the Aeronautical Sciences.

Versteeg, H.K. and Malalasekera, W., 2007. *An introduction to computational fluid dynamics: the finite volume method*. Pearson education.

Walters, D.K. and Cokljat, D., 2008. "A three-equation eddy-viscosity model for reynolds-averaged navier–stokes simulations of transitional flow". *Journal of fluids engineering*, Vol. 130, No. 12.

Wang, X., Zhu, T., Xu, X., Shi, Y., Qiu, H. and Pan, M., 2017. "Fabrication, calibration and proof experiments in hypersonic wind tunnel for a novel mems skin friction sensor". *Microsystem Technologies*, Vol. 23, pp. 3601—-3611. doi:10.1007/s00542-016-3185-8.

White, F. and Christoph, G., 1971. "A simple new analysis of compressible turbulent two-dimensional skin friction under arbitrary conditions". Technical report, RHODE ISLAND UNIV KINGSTON DEPT OF MECHANICAL ENGINEERING AND APPLIED MECHANICS. AFFDL-TR-70-133.

8. RESPONSIBILITY NOTICE

The authors are solely responsible for the printed material included in this paper.